

Mapping of radial velocity component in Taylor Couette flow with Ultrasound Doppler Velocimetry (UVP)

L. Pokorny, Y. Takeda and E.J. Windhab

Laboratory of Food Process Engineering, Institute of Food, Nutrition and Health
ETH Zurich, Schmelzbergstrasse 9, 8092 Zurich, Switzerland



An experimental study of flow characterization in a Taylor–Couette system was made by investigating the radial velocity component by Ultrasonic Doppler Velocimetry based flow mapping (UVP-map). With the technique presented in this work, it is possible to measure the radial velocity components for variable of the axial position in a Couette cell within Taylor vortex flow (TVF), wavy vortex flow (WVF) and spiral vortex domains. The resulting r - z - maps for the different flow states show the location of vortices in the annular gap between the inner and outer cylinder. In the present study, cylindrical and conical concentrically rotating inner bodies were applied a respective flow patterns analyzed. The method uses an additional stroboscopic triggering to synchronize flow measurements and rotational body motion. The fluctuation frequency (f) of unsteady motion in WVF and spiral vortices can be obtained from the power spectrum of velocity. For this, the sampling time period of pulses Δt is calculated from the reciprocal rotational frequency ($\Delta t = 1/f$). The UVP transducer was preferably positioned in radial direction, normal to the surface of the inner rotating body for measuring the radial velocity component. At the same time, the transducer was moved with constant velocity vertically along the outer cylinder height. Accordingly the total measuring time corresponded to the ratio of cylinder height and velocity.

Keywords: UVP flow mapping, Taylor-Couette flow, Wavy Vortex flow, Spiral vortex flow, Couette cell, conical rotor, sampling time of pulses

1 INTRODUCTION

The aim of this study is to develop a method for the localization of flow instabilities that can be used in food industry. These flow instabilities help during filtration to clean the surface of the membrane by removing particle accumulations that makes the filtration process inefficient. Therefore a precise localization is highly important. The benefit of using UVP for this application is its ability to measure turbid systems, mostly present in food industry. The flow structure in Couette cells is well known and therefore the first geometry for the method development [1-6]. By the rotation of the inner cylinder and exceeding a critical Taylor number, Taylor vortices can be formed [1]. When exceeding a second critical rotational speed, various wavy modes are initiated and then change to turbulent Taylor vortex flow. For the best removal of deposited during filtration, vertical movement by wavy vortices or spirals is favored. Analysis and localization of Taylor vortices and turbulent flow are complex because of unsteady flow behavior in the annular gap [2].

Different techniques are described in literature for the analysis of flow structure. Takeda [3] performed UVP measurements for the quantification of Taylor-Couette flow (TCF) for axial velocity profiles. Different publications can be found using Particle Imaging Velocimetry (PIV) for flow visualizations in Couette cell [4-8]. Simulations are based on these measurements leading to the numerical analysis of vertical and radial flow components. In the present

work, the knowledge from former studies will be picked up and further investigated to map the radial flow depending on vertical position for Taylor and wavy vortices and spirals.

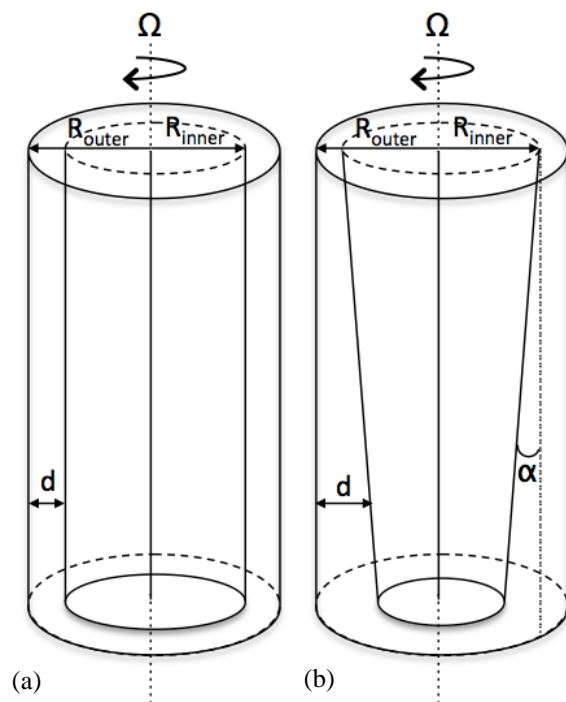


Figure 1: Illustration of the experimental setup for flow structure measurements of silicone oil in Couette cell. (left) regular cylinder, (right) conical cylinder. R_{outer} is the outer cylinder, R_{inner} is the inner cylinder, $d = R_{\text{outer}} - R_{\text{inner}}$, α is the cone angle

2 EXPERIMENTAL

2.1 Regular rotating cylinder setup

A Couette cell constructed by Müller-Fischer et al. [9] allows adjusting the cross-section of the gap between concentric cylinders. The experimental setup (Figure 1a) in the present study consists of a non-transparent inner PVC cylinder (118 mm diameter = $2 \cdot R_{\text{inner}}$, 250 mm height = L) surrounded by a static transparent cylinder (139 mm inner diameter = $2 \cdot R_{\text{outer}}$, 300 mm = L). Thus, the gap-width is $d = 10.5$ mm, the aspect ratio $\Gamma = d/L$ equals 23.5 and the radius ratio $\eta = R_{\text{inner}}/R_{\text{outer}}$ is 0.848. The critical rotational Reynolds number for Taylor-Vortex Flow (TVF) is calculated to 105. The inner cylinder was coupled to a motor, which was controlled by a speed inverter (IKA, Staufen, Germany). The gap space between inner and outer cylinder was filled with the fluid systems to be measured.

2.2 Conical rotor setup

As second configuration, a conical inner rotor was used (Figure 1b) made of non-transparent PVC and inserted into a transparent PVC cylinder (139 mm inner diameter, 300 mm height). The largest rotor diameter was kept at 118 mm (at the top). The cone angle of the conical rotor was adjusted to 10° , resulting in a minimal inner diameter of 30mm (bottom). The radius ratio changed from $\eta = 0.848$ -

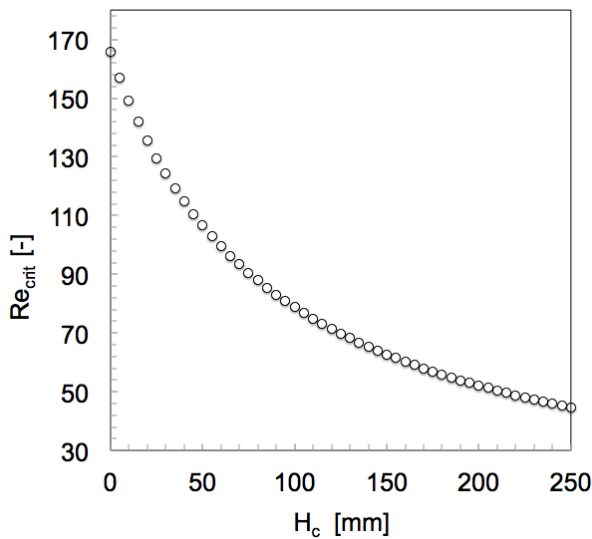


Figure 2: Critical Reynolds number (Re_{crit}) along the height of the conical rotor (H_c)

0.216, whereat the aspect ratio is reduced from $\Gamma = 23.5$ to 0, where 0 represents the bottom part. In figure 2, the critical Reynolds number is presented depending on the local position of the cone resulting in different flow regimes along the axis. These values are theoretical values adapted from Swinney and Gollub [10]. The set-up was kept the same for both rotor configurations described in Section 2.1.

2.3 Fluid systems for flow analysis

In the present work, silicone oil (AK 50, Wacker) was used to investigate the flow structure of Newtonian fluids in the flow cell. Silicone AK 50 oil is a linear, non-reactive polydimethylsiloxane and has a density of 0.96 g/cm^3 , with a kinematic viscosity of $48 \text{ mm}^2/\text{s}$. Polyamid tracer particles with a size of $90 \mu\text{m}$ and a density of 1.03 g/cm^3 (PSP, Met-Flow) were added to the silicon oil with a fraction of ≈ 0.1 wt.% for the UVP measurements.

2.4 Instrumentation - UVP

An UVP-Duo instrument (Met-Flow SA, Lausanne, Switzerland) was used to measure the velocity profiles in the flow cell. An ultrasound transducer with 4 MHz basic frequency and 5 mm active and 8 mm housing diameter (Imasonic) was used. The velocity of sound in the silicone oil was measured to be 1350 m/s at 25°C . Further settings are described in Table 1.

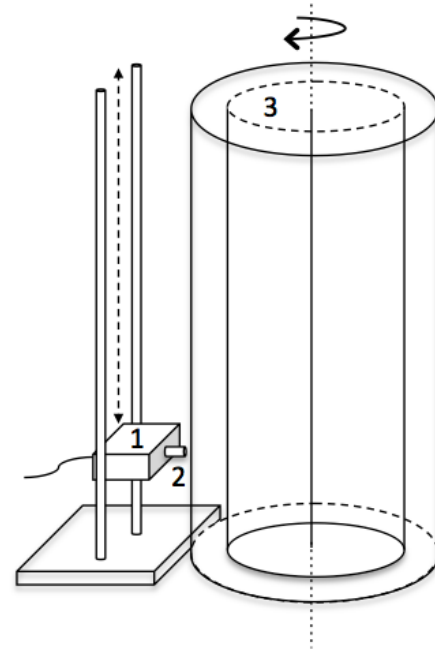


Figure 3: Setup for measuring radial and axial velocity components. (1) transducer holder for positioning, (2) transducer normal to cylinder surface, (3) concentric cylinder.

Table 1: Setting for the UVP measurements

PRF	1.8 kHz
Distance between channels	1.52 mm
Cycles per pulse	4
Position of 1. channel	3.71 mm
Amplification (gain)	6-9

The transducer was fixed in a metal holder (Figure 3), which moved the transducer axially by use of a precision spindle drive. The transducer was positioned starting at the bottom of the outer

cylinder with an angle of 90° to the tangential plane and coupled by a layer of US-wave guiding gel. The metal holder was moved with a constant speed of 0.4 mm/s.

Radial flow components were measured as function of the r and z coordinates as described in further detail in the next paragraph.

2.5 Procedure

Analysis of Taylor-Couette flow (TCF) in concentric cylinder setup

Above the critical Reynolds number TVF appears, which is characterized by the typical axisymmetric toroid shaped vortices. For detailed mapping of the flow structure, it was important to set the minimal sampling time possible and move the transducer along the height with constant speed. Slower upward speed of the transducer, allowed for a better resolution for the velocity map output.

Analysis of wavy vortex flow (WVF) in concentric cylinder setup

With increasing Reynolds number, the Taylor vortices start oscillating. The flow pattern in this domain denotes Wavy Vortex Flow (WVF), in which a travelling wave is superimposed to the TVF leading to flow instability with increased spatio-temporal complexity [1]. By using a strobe

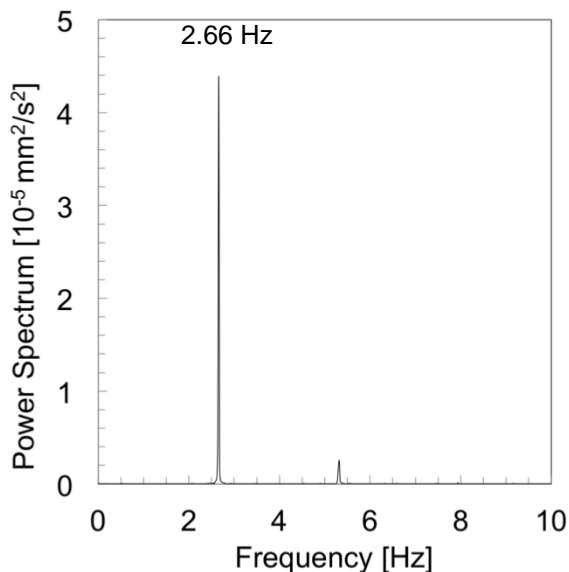


Figure 4: Power spectrum for WVF analysis ($Re=153$). Sampling time was adapted ($\Delta t = 1/f = 1/2.66 = 376$ ms).

synchronized to the rpm this oscillating wave can be "virtually frozen". Accordingly the sampling time of the recorded pulses Δt was adapted to the frequency of the wave oscillation f ($\Delta t = 1/f$) or proportional to the rpm respectively. The corresponding frequency was obtained from the measurement of the radial velocity pattern at a fixed axial transducer position at half of the cylindrical

height. The power spectrum in Figure 4 shows the frequency of the oscillation. Further investigations will be performed concerning the wavy frequency and sampling time.

Analysis of Spiral Vortex Flow (SVF) for conical

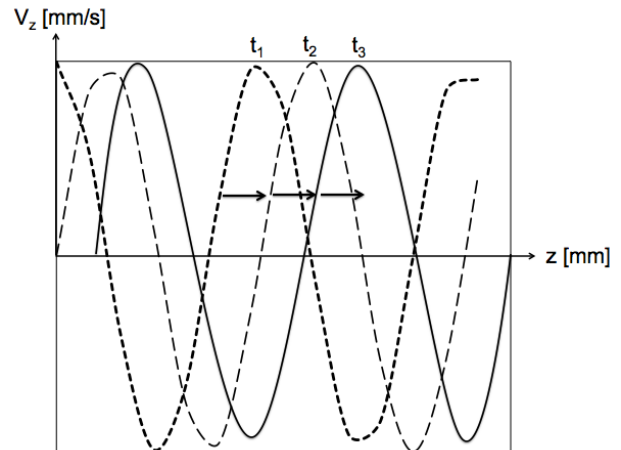


Figure 5: Drifting of axial velocity used for the calculation of sampling time from axial travelling speed. V_z = velocity, z = position, t = time,

inner rotor

In the annular gap of the conical rotor, spiral waves were observed [11]. The vortices travelled along the rotor axis with a distinct speed depending on the angle of the cone. The axial travelling speed was obtained by measuring additionally the axial velocity profile in the direction of the gap (centerline) from the top. The sampling time Δt was adapted until the drifting motion was compensated in the velocity plot (Figure 5). With the adapted sampling time, the transducer was moved axially with a constant speed of 0.4 mm/s.

3 RESULTS AND DISCUSSION

3.1 TVF and WVF in concentric cylinder setup

The results for TVF and WVF obtained by the adaptation of the sampling time interval Δt are presented in Figure 6. The black and white structures represent the negative and positive radial velocity domains, respectively. The length of the map corresponds to the height of the cylinder and the width shows the cylinder gap between inner and outer cylinder. The structure for the WVF was



Figure 6: Vortex structure in annular gap for TVF $Re = 126$ (above) and with WVF $Re=153$ (below). Black = negative velocity, white = positive velocity, upper part = inner gap width, lower part = outer gap width

obtained by adjusting the sampling time to the frequency of $f = 2.66$ Hz resulting in $\Delta t = 376$ ms.

The map for TVF is regular and independent of the position, whereas for the WVF an irregular structure is superimposed as a consequence of the wavy motion.

3.2 Spiral Vortex Flow in conical rotor setup

Figure 7 shows a map for spiral vortex flow formation in the conical rotor setup. The frequency of travelling vortices was measured as $f = 0.3$ Hz resulting in a sampling time of 2.7s. The axial motion of travelling vortices could be matched by the strobe technique applied. It is important to

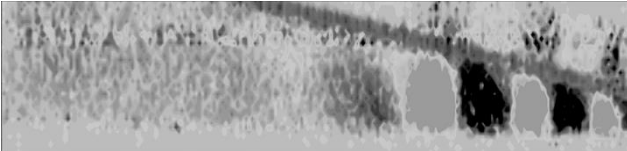


Figure 7: Spirals vortex flow with conical shaped rotor c , above the critical Reynolds number for the upper part of the setup. Frequency of axial spiral motion $f = 0.3$ Hz, $\Delta t = 2.7$ s. Black = negative velocities, white = positive velocities

notice, that in case of spiral vortices, no oscillating character was observed, however instead a drifting frequency was detected resulting in an “out-flushing” of the vortices at increasing gap width. Further investigations have to be performed in order to better characterize the spiral vortex flow structure with the introduced technique.

4 CONCLUSIONS

In this study, a method was developed to improve the mapping of flow fields of TVF, WVF and SWF in concentric cylindrical and conical annular rotor/stator gaps applying a stroboscopic technique. The flow of silicone oil was analyzed in such cylindrical and conical concentric gaps, with inner rotor. The respective velocity profiles were obtained using an ultrasonic velocity profiler (UVP, Metflow). The transducer was radially oriented and simultaneously moved in the axial z -direction (along the gap height). With adjusting the sampling time intervals UVP pulses to the frequency of the wavy or spiral vortex motion, precise velocity profiles snap-shots were received.

This novel application for UVP allows accurate mapping of the TVF, WVF and SWF velocity profiles in z - and r -directions as a function of time. Related velocity maps were compiled successfully for TVF, WVF and SVF. This will help in different application of such flow characteristics for the quantitative determination and localization of respective flow characteristics and thus improve conditions for

designing and scaling of related processes.

5 ACKNOWLEDGEMENTS

D. Dufour for introduction into UVP measuring principles; D. Kiechl and B. Pfister for construction of the experimental setup and B. Koller for giving a helpful IT-support.

REFERENCES

- [1] Taylor, G.I. (1923). "Stability of a Viscous Liquid contained between Two Rotating Cylinders". *Phil. Trans. Royal Society A223* (605–615): 289–343.
- [2] Andereck, C.D., Liu, S.S., Swinney, H.L. (1986). "Flow regimes in a circular Couette system with independently rotating cylinders." *Journal of Fluid Mechanics*, 164, 155-183.
- [3] Takeda, Y. (1999). "Quasi-periodic state and transition to turbulence in a rotating Couette system." *Journal of Fluid Mechanics*, 389(1), 81–99.
- [4] Conway, S.L, Shinbrot, T., Glasser, B.J. (2004). "A Taylor vortex analogy in granular flows", *Nature*, 431, 433-437.
- [5] Wereley, S.T., Lueptow, R.M. (1998). "Spatio-temporal character of non-wavy and wavy Taylor–Couette flow." *Journal of Fluid Mechanics*, 364, 59-80.
- [6] Wereley, S.T., Lueptow, R.M. (1999). "Velocity field for Taylor–Couette flow with an axial flow." *Physics of Fluids*, 11(12), 3637-3649.
- [7] Abcha, N., Latrache, N., Dumouchel, F., Mutabazi, I. (2008). "Qualitative relation between reflected light intensity by Kalliroscope flakes and velocity field in the Couette–Taylor flow system." *Experiments in Fluids*, 45(1), 85-94.
- [8] Hwang, J.Y., Yang, K.S. (2004). "Numerical study of Taylor–Couette flow with an axial flow." *Computers & Fluids*, 33(1), 97–118.
- [9] Müller-Fischer, N. (2007). "Dynamically Enhanced membrane foaming." *Food Process Engineering Dissertation, Laboratory of Food Process Engineering, ETH Zürich, Vol. 28, ISBN: 3-905609-32-0.*
- [10] Swinney, H.L. and Gollub, J.P. (1981). "Hydrodynamic Instabilities and the Transition to Turbulence. *Topics in Applied Physics* 45, 292 S., ISBN: 3-540-10390-2.
- [11] Wimmer, M. (1992). "Vortex patterns between cones and cylinders. In: *Ordered and Turbulent Patterns in Taylor-Couette Flow.*" *NATO ASI Series*, 297, 205-211.